Topological Methods for Flow Visualization

Gerik Scheuermann and Xavier Tricoche
University of Kaiserslautern, Germany

Abstract

Numerical simulations provide scientists and engineers with an increasing amount of vector and tensor data. The visualization of these large multivariate datasets is therefore a challenging task. Topological methods efficiently extract the structure of the corresponding fields to come up with an accurate and synthetic depiction of the underlying flow. This approach takes its roots and inspiration in the visionary work of Poincaré at the end of the 19th century. Practically, it consists in partitioning the domain of study into subregions of homogeneous qualitative behavior. Extracting and visualizing the corresponding graph permits to convey the most meaningful properties of multivariate datasets. This has motivated the design of various topology-based visualization schemes. This chapter proposes an introduction to the theoretical foundations of the topological approach and presents an overview of the corresponding visualization methods. Emphasis is put on recent advances. In particular, the processing of turbulent or unsteady vector and tensor fields is addressed.

1 Introduction

Vector and tensor fields are traditionally objects of major interest for visualization. They are the mathematical language of many research and engineering areas like e.g. fundamental physics, optics, solid mechanics or fluid dynamics but also civil engineering, aeronautics, turbomachinery or weather forecast. Vector variables are in this context velocity, vorticity, magnetic or electric field, a force or the gradient of some scalar field like e.g. temperature. Tensor variables might correspond to stress, strain or rate of deformation, for instance. From a theoretical viewpoint, vector and tensor fields have received much attention from mathematicians, leading to a precise and rigorous framework that constitutes the basis of specific visualization methods. Of particular interest is Poincaré's work [20] that laid down the foundations of a geometric interpretation of vector fields associated to dynamical systems at the end of the 19th century: the analysis of the phase portrait provides an efficient and aesthetic way to apprehend the information contained in abtract vector data. Nowadays, following this theoretical inheritance, scientists typically focus their study on the topology of vector and tensor datasets provided by Computational Fluid Dynamics (CFD) or Finite Elemente Methods. A typical and very

active application field is fluid dynamics where complex structural behaviors are investigated in the light of their topology [14, 27, 19, 3]. It was shown for instance that topological features are directly involved in crucial aspects of flight stability like flow separation or vortex genesis [4]. Informally, the topology is the qualitative structure of a multivariate field. It leads to a partition of the domain of interest into subdomains of equivalent qualitative nature. Therefore, extracting and studying this structure permits to focus the analysis on essential properties. For visualization purposes, the depiction of the topology results in synthetic representations that transcribe the fundamental characteristics of the data. Moreover it permits fast extraction of global flow structures that are directly related to features of interest in various practical applications. Further, topology-based visualization results in a dramatic decrease in the amount of data necessary for interpretation which makes it very appealing for the analysis of large scale datasets. These ideas are at the basis of the topological approach that has gained an increasing interest in the visualization community during the last decade. First introduced for planar vector fields by Helman and Hesselink [9], the basic technique has been continuously extended since then. A significant milestone on this way was the work of Delmarcelle [5] that transposed the original vector method to symmetric, second-order tensor fields.

The contents of this survey are organized as follows. Vector fields are first considered. Basic theoretical notions are introduced in section 2. They result from the qualitative theory of dynamical systems, initiated by Poincaré's work. Nonlinear and parameter-dependent topologies are discussed along with the fundamental concept of bifurcation. Tensor fields are treated in section 3. Following Delmarcelle's approach, we are concerned with the topology of the eigenvector fields of symmetric, second-order tensor fields. It is shown that they induce line fields in which tangential curves can be computed, analogous to streamlines for vector fields. We explain how singularities are defined and characterized and how bifurcations affect them in the case of unsteady tensor fields. This completes the framework required for the description of topology-based visualization of vector and tensor fields in section 4. The presentation covers original methods for 2D and 3D fields, extraction and visualization of non-linear topology, topology simplification for the processing of turbulent flows and topology tracking for parameter-dependent datasets. Finally, section 5 completes the presentation in addressing open questions and suggesting future research directions to extend the scope of topology-based visualization.

2 Vector Field Topology

In the following, we propose a short overview of the theoretical framework of vector field topology, which we restrict to the requirements of visualization techniques.

2.1 Basic Definitions

We consider a vector field $\boldsymbol{v} : U \subseteq \mathbb{R}^n \times \mathbb{R} \to T\mathbb{R}^n \simeq \mathbb{R}^n$, that is a vector valued function that depends on a space variable and on an additional scalar parameter, say time. The vector field $\boldsymbol{v}$ generates a *flow* $\boldsymbol{\phi}_t : U \subseteq \mathbb{R}^n \to \mathbb{R}^n$, where $\boldsymbol{\phi}_t := \boldsymbol{\phi}(\boldsymbol{x}, t)$ is a smooth function defined for $(\boldsymbol{x}, t) \in U \times (I \subseteq \mathbb{R})$ satisfying

$$\left.\frac{d}{dt}\boldsymbol{\phi}(\boldsymbol{x}, t)\right|_{t=\tau} = \boldsymbol{v}(\tau, \boldsymbol{\phi}(\boldsymbol{x}, \tau))$$

for all $(\boldsymbol{x}, \tau) \in U \times I$. Practically we limit our presentation to the case $n = 2$ or 3 in the following. The function $\boldsymbol{\phi}(\boldsymbol{x}_0, .) : t \mapsto \boldsymbol{\phi}(\boldsymbol{x}_0, t)$ is an *integral curve* through $\boldsymbol{x}_0$. Observe that existence and uniqueness of integral curves are ensured under the assumption of fairly general continuity properties of the vector field. In the special but fundamental case of steady vector fields, i.e. fields that do not depend on the variable t, integral curves are called *streamlines*. Otherwise, they are called *path lines*. The uniqueness property guaranties that streamlines cannot intersect in general. The set of all integral curves is called *phase portrait*, according to Poincaré's original formalism. The qualitative structure of the phase portrait is called topology of the vector field. First we focus on the steady case and consider next parameter-dependent topology.

2.2 Steady Vector Fields

The local geometry of the phase portrait is characterized by the nature and position of its *critical points*. In the steady case, these *singularities* are locations where the vector field is zero. Consequently, they behave as 0D integral curves. Furthermore they are the only positions where streamlines can intersect (asymptotically). Basically, the qualitative study of critical points relies on the properties of the Jacobian matrix of the vector field at their position. If the Jacobian has full rank, the critical point is said to be linear or of *first order*. Otherwise, a critical point is of *higher order*. Next we discuss the planar and three-dimensional case successively. Observe that considerations made for 2D vector fields also apply to vectors field defined over a 2D manifold embedded in 3D like for example the surface of an object surrounded by a 3D flow.

Planar case. Planar critical points have benefited from much attention from mathematicians. A complete classification has been provided by Andronov et al. [1]. Additional excellent references are [2] and [12]. Depending on the real and imaginary parts of the eigenvalues, linear critical points may exhibit the configurations shown in Fig. 1. Repelling singularities act as *sources* whereas attracting ones are *sinks*. *Hyperbolic* critical points are a subclass of linear singularities for which both eigenvalues have non zero real part. Thus a center is non-hyperbolic. The analysis of non-linear critical points, on the contrary, requires to take into account higher-order polynomial terms in the Taylor expansion. Their vicinity is decomposed into

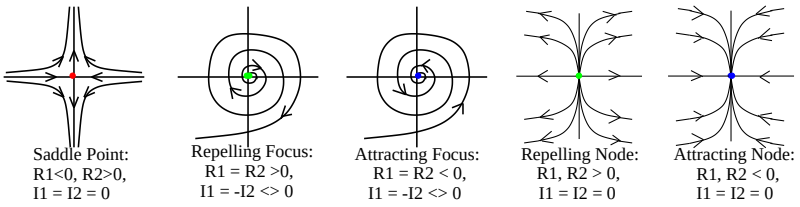

Figure 1: Basic configurations of 1st-order planar critical points

an arbitrary combination of *hyperbolic*, *parabolic* and *elliptic* curvilinear sectors, see Fig. 2. The bounding curve of a hyperbolic sector is called *separatrix*. Back in the

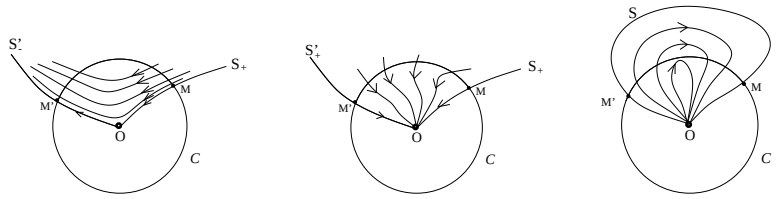

(a) Hyperbolic (b) Parabolic (c) Elliptic

Figure 2: Sector types of arbitrary planar critical points

linear case, separatrices only exist for saddle points where they are the four curves that reach, forward or backward in time, the singularity. Thus we obtain a simple definition of planar topology as the graph whose vertices are the critical points and whose edges are the separatrices integrated away from the corresponding singularities. This needs to be completed by *closed orbits* that are periodic integral curves. Closed orbits play the role of sources or sinks and can be seen as additional separatrices. It follows that topology decomposes a vector field into subregions where all integral curves have a similar asymptotic behavior: they converge toward the same critical point (resp. closed orbit) both forwards and backwards. We complete our overview of steady planar topology by mentioning the *index* of a critical point introduced by Poincaré in the qualitative theory of dynamical systems. It measures the number of field rotations along a closed curve that is chosen arbitrarily small around the critical point. By continuity of the vector field this is always a (signed) integer value. The index is an invariant quantity for the vector field and possesses several properties that explain its importance in practice. Among them we have: *a*. the index of a curve that encloses no critical point is zero, *b*. The index of a linear critical point is -1 for a saddle point and +1 for every other type (see Fig. 3), *c*. the index of a closed orbit is always +1, *d*. the index of a curve enclosing several critical points is the sum of their individual indices.

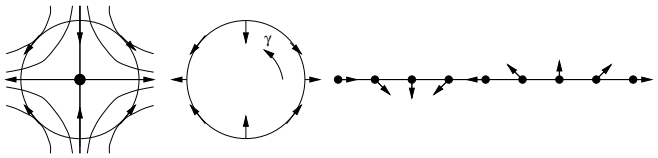

Figure 3: Simple closed curve of index -1 (saddle point)

Three-dimensional case. The three-dimensional case lacks an analogous intensive theoretical treatment. To our knowledge there exists no exhaustive characterization of arbitrary three-dimensional critical points, i.e. no generalization to 3D of the sector type decomposition achieved by Andronov. Therefore we only address linear 3D critical points. Alike the planar case, the analysis is based on the eigenvalues of the Jacobian. There are two main possibilities: the eigenvalues are either all real or two of them are complex conjugate, see [2].

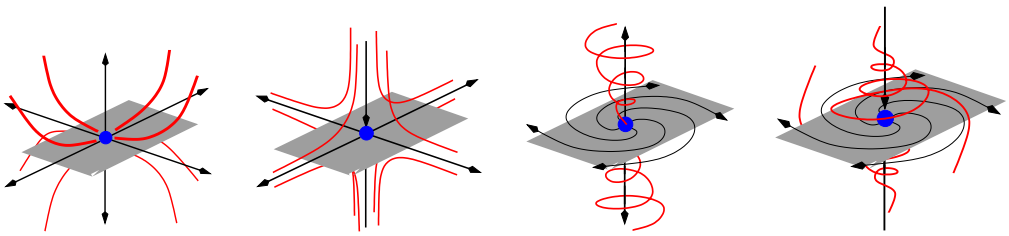

(a) 3D node (b) node saddle (c) 3D spiral (d) spiral saddle

Figure 4: Linear 3D critical points

- *Three real eigenvalues.* One has to distinguish the case where all three eigenvalues have the same sign, in which case we have a (either attracting or repelling) 3D node, and the case where only two eigenvalues have the same sign: the two eigenvectors associated with the eigenvalues of same sign span a plane in which the vector field behaves as a 2D node and the critical point is a 3D saddle.
- *Two complex eigenvalues.* Once again there are two possibilities. If the common real part of both complex eigenvalues has the same sign as the real eigenvalue, one has a 3D spiral, i.e. a (either attracting or repelling) critical point that exhibits a 2D spiral structure in the plane spanned by the eigenspace related to the complex eigenvalues. If not, one has a second kind of 3D saddle.

Refer to Fig. 4 for a visual impression. Analoguous to the planar case, a critical point is called *hyperbolic* in this context if the eigenvalues of the Jacobian have all non-zero real parts. Compared to 2D critical points, separatrices in 3D are not restricted to

curves but can be surfaces, too. These surfaces are called stream surfaces and are constituted by the set of all streamlines that are integrated from a curve. The linear 3D topology is thus composed of nodes, spirals and saddles that are interconnected by curve and surface separatrices emanating from saddle points. These are in fact the eigenspaces corresponding to the eigenvalues with positive, resp. negative real part, started in the vicinity of the critical point and integrated away. Depending on the considered type, repelling and attracting eigenspaces can be 1D or 2D, leading to curves and surfaces, see Fig. 4(b) and Fig. 4(d).

2.3 Parameter-Dependent Vector Fields

The previous sections focused on steady vector fields. Now, if the considered vector field depends on an additional parameter, the structure of the phase portrait may transform as the value of this parameter evolves: position and nature of critical points can change along with the connectivity of the topological graph. These modifications - called *bifurcations* in the literature - are continuous evolutions that bring the topology from a stable state to another, structurally consistent, stable state. Bifurcations have been the subject of an intensive research effort in pure and applied mathematics [7]. The present section intends to provide a short introduction to these notions. Notice that the treatment of 3D bifurcations is beyond the scope of this paper since they have not been applied to flow visualization up to now. We start with basic considerations about structural stability and then describe typical planar bifurcations.

Structural stability. As said previously, bifurcations consist in topological transitions between stable structures. In fact, the definition of structural stability involves the notion of structural equivalence: Two vector fields are said to be *equivalent* if there exists a diffeomorphism (i.e. a smooth map with smooth inverse) which takes the integral curves of one vector field to those of the second while preserving orientation. *Structural stability* is now defined as follows: the topology of a vector field $\boldsymbol{v}$ is stable if any perturbation of $\boldsymbol{v}$, chosen small enough, results in a vector field that is structurally equivalent to $\boldsymbol{v}$. We can now state a simplified version of the fundamental Peixoto's theorem [7] on structural stability for two-dimensional flows. *A smooth vector field on a two-dimensional compact planar domain of $\mathbb{R}^2$ is structurally stable iff the number of critical points and closed orbits is finite and each is hyperbolic, and if there are no integral curves connecting saddle points.* Practically, Peixoto's theorem implies that a planar vector field typically presents saddle points, sinks and sources as well as attracting or repelling closed orbits. Furthermore, it asserts that non-hyperbolic critical points or closed orbits are unstable because small perturbations can make them hyperbolic. Saddle connections, as far as they are concerned, can be broken by small perturbations as well.

Bifurcations. One distinguishes two types of structural transitions: local and global bifurcations.

Local Bifurcations. There are two main types of local bifurcations affecting the nature of a singular point in 2D vector fields. The first one is the so-called *Hopf bifurcation*. It consists in the transition from a sink to a source with simultaneous emission of a surrounding closed orbit that behaves as a sink, preserving local consistency with respect to the original configuration, see Fig. 5. At the bifurcation point there is a center. The reverse evolution is possible too, as well as an inverted role of sinks and sources. A second typical local bifurcation is called *Fold Bifurcation* and

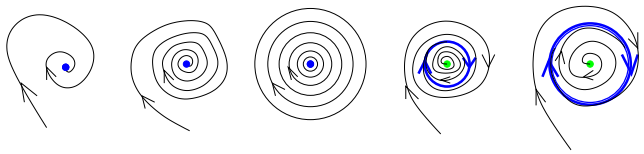

Figure 5: Hopf bifurcation

consists in the pairwise annihilation or creation of a saddle and a sink (resp. source). This evolution is depicted in Fig. 6. Observe that the index of the concerned region remains 0 throughout the transformation.

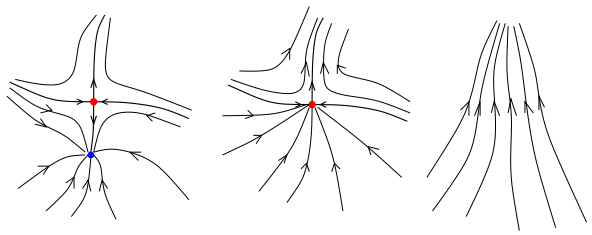

Figure 6: Pairwise annihilation

Global Bifurcations. As opposed to the cases mentioned above, global bifurcations do not take place in a small neighborhood of a singularity but entail significant changes in the flow structure and involve large domains by modifying the connectivity of the topological graph. Actually, global bifurcations still remain a challenging topic for mathematicians. Consequently, we just mention here a typical configuration exhibited by such transitions: the unstable saddle-saddle connection (c.f. Peixoto's theorem). This is the central constituent of *basin bifurcations* where the relative position of two separatrices emanating from two neighboring saddle points are swapped through a saddle-saddle separatrix.

3 Tensor Field Topology

Making use of the results obtained for vector fields, we now turn to tensor field topology. We adopt for our presentation a similar approach as the original work of Delmarcelle [5, 6] and focus on symmetric second-order real tensor fields that we

analyze through their eigenvector fields. We seek here a framework that permits to extend the results discussed previously to tensor fields. However, since most of the research done so far has been concerned with the 2D case, we put the emphasis on planar tensor fields and point out the generalization to three-dimensional fields. A mathematical treatment of these notions can be found in [28] where it is shown how covering spaces permit to associate a line field with a vector field. In this section, we first introduce useful notations in the steady case and show how symmetric second-order tensor fields can be interpreted as line fields. This makes the integration of tangential curves called tensor lines possible. Next, singularities are considered. We complete the presentation with tensor bifurcations.

3.1 Line Fields

Basic definitions. In the following, we call tensor a symmetric second-order real tensor of dimension 2 or 3. This is a geometric invariant that corresponds to a linear transformation and can be represented by a matrix in a cartesian basis. By extension, we define a tensor field as a map T that associates every position of a subset of the euclidean space $\mathbb{R}^n$ with a $n \times n$ symmetric matrix. Thus, it is characterized by $\frac{1}{2}n(n+1)$ independent, real scalar functions. Remark that an arbitrary second-order tensor field can always be decomposed into its symmetric and anti-symmetric parts. From the structural point of view, a tensor field is fully characterized by its *deviator field* which is obtained by substracting from the tensor its isotropic part, that is $\mathrm{D} = \mathrm{T} - \frac{1}{n}\ (\mathrm{tr\ T})\mathrm{I}_n$, where tr T is the trace of T and I_n the identity matrix in $\mathbb{R}^n$. Observe that the deviator has trace zero by definition. The analysis of a tensor field is based on the properties of its eigensystem. Since we consider symmetric tensors, the eigenvectors always form an orthogonal basis of $\mathbb{R}^n$ and the eigenvalues are real. It is a well-known fact that eigenvectors are defined modulo a non-zero scalar which means that they have neither inherent norm nor orientation. This characteristic plays a fundamental role in the following. Through its corresponding eigensystem, any symmetric real tensor field can now be associated with a set of orthogonal eigenvector fields. We choose the following notations in 3D. *Let $\lambda_1 > \lambda_2 > \lambda_3$ be the real eigenvalues of the symmetric tensor field* $\mathbf{T}$ *(i.e. λ_1, λ_2 and λ_3 are scalar fields as functions of the coordinate vector $\boldsymbol{x}$). The corresponding eigenvector fields $\boldsymbol{e}_1$, $\boldsymbol{e}_2$ and $\boldsymbol{e}_3$ are respectively called* major, medium *and* minor eigenvector field. In the 2D case, there are just major and minor eigenvectors. We now come to tensor lines that are the object of our structural analysis.

Tensor lines. A *tensor line* computed in a Lipschitz continuous eigenvector field, is a curve that is everywhere tangent to the direction of the field. Because of the lack of both norm and orientation, the tangency is expressed at each position in the domain in terms of lines. For this reason, an eigenvector field corresponds to a *line field*. Nevertheless, except at positions where two (or three) eigenvalues are equal, integration can be carried out in a way similar to streamlines for vector fields by choosing an arbitrary local orientation. Practically, this consists in determining a

continuous angular function θ^* defined modulo 2π that is everywhere equal to the angular coordinate θ of the line field, modulo π. Considering the set of all tensor lines as a whole, the topology of a tensor field is defined as the structure of the tensor lines. It is interesting to observe that the topologies of the different eigenvector fields can be deduced from another through the orthogonality of the corresponding line fields.

3.2 Degenerate points

The inconsistency in the local determination of an orientation as described previously only occurs in the neighborhood of positions where several eigenvalues are equal. There, the eigenspaces associated with the corresponding eigenvalues are no longer one-dimensional. For this reason, such positions are singularities of the line field. To remain consistent with the notations originally used by Delmarcelle, we call them *degenerate points* though they are typically called *umbilic points* in differential geometry. Because of the direction indeterminacy at degenerate points, tensor lines can meet there, which underlines the analogy with critical points.

Planar case. The deviator part of a 2D tensor field is zero if and only if both eigenvalues are equal. For this reason, degenerate points correspond to zero values of the deviator field. Thus D can be approximated as follows in the vicinity of the degenerate point P_0.

$$\mathrm{D}(P_0 + d\boldsymbol{x}) = \nabla\mathrm{D}(P_0)d\boldsymbol{x} \; + \; o(d\boldsymbol{x}),$$

where $d\boldsymbol{x} = (x, y)^T$, and with α and β being real scalar functions on $\mathbb{R}^2$

$$\mathrm{D}(x,y) \; = \; \begin{pmatrix} \alpha & \beta \\ \beta & -\alpha \end{pmatrix}, \text{ and } \nabla\mathrm{D}(P_0)d\boldsymbol{x} = \begin{pmatrix} \frac{\partial\alpha}{\partial x}dx + \frac{\partial\alpha}{\partial y}dy & \frac{\partial\beta}{\partial x}dx + \frac{\partial\beta}{\partial y}dy \\ \frac{\partial\beta}{\partial x}dx + \frac{\partial\beta}{\partial y}dy & -\frac{\partial\alpha}{\partial x}dx - \frac{\partial\alpha}{\partial y}dy \end{pmatrix}.$$

If the condition $\frac{\partial\alpha}{\partial x}\frac{\partial\beta}{\partial y} - \frac{\partial\alpha}{\partial y}\frac{\partial\beta}{\partial x} \neq 0$ holds, the degenerate point is said to be linear. The local structure of the tensor lines in its vicinity depends on the position and number of radial directions. If θ is the local angle coordinate of a point with respect to the degenerate point, $u = tan\theta$ is solution of the following cubic polynomial

$$\beta_2 u^3 + (\beta_1 + 2\alpha_2)u^2 + (2\alpha_1 - \beta_2)u - \beta_1 = 0,$$

with $\alpha_1 = \frac{\partial\alpha}{\partial x}$, $\alpha_2 = \frac{\partial\alpha}{\partial y}$, same for β_i. This equation has either 1 or 3 real roots that all correspond to angles along which the tensor lines asymptotically reach the singularity. These angles are defined modulo π, so one obtains up to 6 possible angle solutions. Since we limit our discussion to a single (minor / major) eigenvector field, we are finally concerned with up to 3 radial eigenvectors. The possible types of linear degenerate points are trisectors and wedges, see Fig. 7. In fact, the special importance of radial tensor lines is explained by their interpretation as separatrices. As a matter of fact, like critical points, the set of all tensor lines in the vicinity

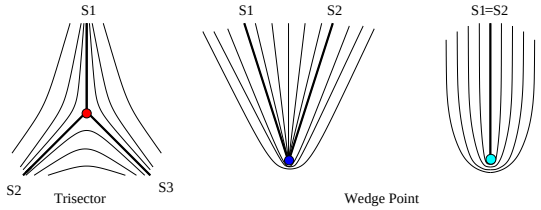

Figure 7: Linear degenerate points in the plane

of a degenerate point is partitioned into hyperbolic, parabolic and elliptic sectors. Separatrices are again defined as the bounding curves of the hyperbolic sectors (compare Fig. 7). In fact, a complete definition of the planar topology involves *closed tensor lines*, too. However, they are rare in practice. The analogy with vector fields may be extended by defining the tensor index of a degenerate point [5, 28] that measures the number of rotations of a particular eigenvector field along a closed curve surrounding a singularity. Notice that tensor indices are half integers, due to orientation indeterminacy: trisectors have index $-\frac{1}{2}$ and wedges have index $\frac{1}{2}$. The nice properties of Poincaré's index extend here in a very intuitive fashion.

Three-dimensional degenerate points. In the three-dimensional case, singularities are of two types: eigenspaces may become two or three dimensional, leading to tangency indeterminacy in the corresponding eigenvector fields. To simplify the presentation, we restrict our considerations to the trace-free deviator $\mathrm{D} = (D_{ij})_{i,j}$. The characteristic equation is $-\lambda^3 + b\lambda + c = 0$, where $-c$ is the determinant of D and $b = \frac{1}{2}\sum_i D_{ii} + \sum_{i<j} D_{ij}^2$. The quantity $\Delta = (\frac{c}{2})^2 - (\frac{b}{3})^3$ determines the number of distinct real roots of the equation: $\Delta < 0$ yields 3 distinct real roots while there are multiple roots iff $\Delta = 0$ (complex conjugate roots are impossible since D is symmetric). Thus, degeneracies correspond to a maximum of Δ which is everywhere negative except at points, lines or surfaces where it is zero. Here a major difference with 3D vector field topology must be underlined: The loci of singularities are not restricted to points. Refer to [11, 16] for additional information.

3.3 Parameter-Dependent Topology

Again, the natural question that arises at this stage is the structural stability of topology under small perturbations of an underlying parameter. We restrict our considerations to the simplest cases in 2D of local and global bifurcations to remain in the scope of the methods to come. The observations proposed next are all inspired by geometric considerations.

Following the basic idea behind Peixoto's theorem, we see that the only stable degenerate points must be the linear ones. As a matter of fact the asymptotic behavior of tensor lines in the vicinity of a degenerate point is determined by the third-order differential ∇D (thus leading to a linear degenerate point) except at locations where it becomes singular. This is by essence an unstable property since arbitrary small

perturbations in the coefficients lead to one of the linear configurations. Continuing our analogy with the vector case, we conclude that integral curves are unstable if they are separatrices for both degeneracies they link together. This is because a small angle perturbation of the line field around any point along the separatrix suffices to break the connection. Using these elementary results, we review typical planar bifurcations.

Pairwise creation and annihilation. Since a wedge and a trisector have opposite indices, a closed curve enclosing them has index 0. This simple fact is the basic idea behind pairwise creations or annihilations. Indeed, the zero index computed along this closed curve shows that the combination of both degenerate points is structurally equivalent to a uniform flow. Therefore, a wedge and a trisector can merge and disappear: this is a *pairwise annihilation*. The reverse evolution is called a *pairwise creation*. Both are the equivalent of the fold bifurcations for critical points. An example is proposed in Fig. 8.

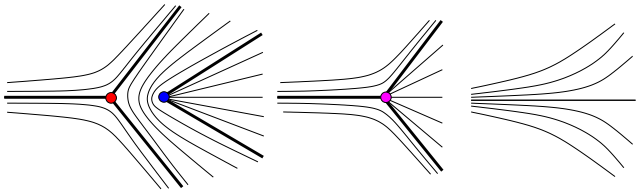

Figure 8: Pairwise annihilation of degenerate points

Homogeneous mergings. When two linear degenerate points of same nature merge, their half-integer indices are added and the resulting singularity exhibits a pattern corresponding to a linear critical point, e.g. two trisectors lead to a saddle point. However, according to what precedes, these new degenerate points are nonlinear and thus unstable. Details on that topic can be found in [5].

Wedge bifurcation. Both existing types of wedges have the same index $\frac{1}{2}$. As a consequence the transition from one type to the other can take place without modifying structural consistency of the surrounding flow. From a topological viewpoint, this evolution corresponds to the creation (resp. disappearance) of a parabolic sector along with an additional separatrix.

Global bifurcations. To finish this presentation of structural transitions in line fields, we briefly consider the simplest type of global bifurcation. It is intimately related to the unstable separatrices defined above. They occur when the relative position of two separatrices is changed through a common separatrix.

4 Topological Visualization of Vector and Tensor Fields

The theoretical framework described previously has motivated the design of techniques that build the visualization of vector and tensor fields upon the extraction and analysis of their topology. We start with a recall of the original method of Helman and Hesselink for vector fields, later extended by Delmarcelle to symmetric second-order tensor fields. After that, we focus on recent advances in topology-based visualization. New methods designed to complete the visualization of planar steady fields are discussed first. Non-linear topology is addressed next. Techniques for reducing topological complexity in turbulent fields is considered and the presentation ends with the topological visualization of parameter-dependent (e.g. unsteady) datasets. Throughout the presentation, we privilege a simultaneous treatment of vector and tensor techniques, making natural use of the profound theoretical relationships between their topologies.

4.1 Topology Basics

Original methods. Helman and Hesselink pioneered topology-based visualization in 1989 [9]. They proposed a scheme for 2D vector fields, restricting the characterization of critical points to a linear precision. Remember that this leads to a graph where saddles, spirals, and nodes are the vertices and separatrices are the edges, integrated along the eigendirections of the saddle points. They extended their technique to tangential vector fields defined over surfaces embedded in 3D space [10]. Stream surfaces [13, 22] are started along the separatrices. This was shown to permit the visualization of separation and attachment lines in some cases. At the same time, Globus et al. suggested a similar technique to visualize the topology of 3D vector fields defined over curvilinear grids [8]. They do not provide the separating surfaces associated with 3D saddles but use glyphs to depict their structure locally and draw streamlines from them. Observe that all these methods require the integration of streamlines, which is typically carried out with a numerical scheme, e.g. Runge-Kutta with adaptive stepsize, see [21]. Analytical methods exist for piecewise linear vector fields over triangulations, resp. tetrehedrizations [18].
The topological approach for vector fields inspired Delmarcelle who extended the original scheme to symmetric, second-order planar tensor fields [6] within his work on general techniques for tensor field visualization [5]. Here too, analysis is restricted to linear precision. The missing quantitative information carried by eigenvalues is inserted into the representation by means of color-coding. Existing attempts to generalize this method to three-dimensional tensor fields suffer from the inherent difficulty of locating 3D degenerate points [11, 16]. Typically they lead to complicated polynomial systems of high degree and lack surfaces to partition the domain conveniently.

Closed orbits. The original topological method neglects the importance of closed orbits. As said previously, these features play a major role in the flow structure,

acting like sinks or sources and playing the role of additional separatrices. Moreover, they represent a challenging issue for numerical integration schemes used in practice since every streamline that converges toward a closed orbit will result in an endless computation. A traditional but inaccurate way to solve this problem is to limit the number of integration steps. However this does not permit to distinguish a closed orbit from a slowly converging spiral, i.e. a spiral with high vorticity. Furthermore, this might be very inefficient if the number of iterations is set to a fairly large value to avoid a premature integration break. To overcome this deficiency, Wischgoll and Scheuermann first proposed a method that properly identifies and locates closed orbits [34]. Their basic idea is to detect on a cell-wise basis a periodic behaviour during streamline integration. Practically, once a cell-cycle has been infered, a control is carried out over the edges of the concerned cells. This ensures that a streamline entering the cycle will remain trapped. If this condition is met and no critical point is present in the cycle, the Poincaré-Bendixon theorem [7] ensures that a closed orbit is contained in it. Precise location is obtained by looking for a fixed point of the Poincaré map [2]. The method was generalized to 3D in [35]. Remark that the extension to tensor fields is straightforward even if closed tensor lines are rare in practice.

Local topology. The definition of topology given previously does not address specifically vector fields defined over a bounded domain. As a matter of fact, the idea behind topology visualization is to partition the domain into subregions where all streamlines exhibit the same asymptotic behaviour. If the considered domain is infinite, this is equivalent to looking for subregions where all streamlines reach the same critical point both backward and forward. Now, Scientific Visualization is typically concerned with domains spanned by bounded grids. In this case, the boundary must be incorporated in the topology analysis: outflow parts behave as sinks, inflow parts as sources, and the points separating them as half-saddles. Scheuermann et al. proposed a method that identifies these regions along the boundary of planar vector field [23]. It assumes that the restriction of the vector field to the boundary is piecewise linear. Half-saddles are located and separatrices are started there, forward and backward, to complete the local topology visualization. Observe that the same principle can be applied in 3D: half-saddles are no longer points but closed curves from which stream surfaces can be drawn.

4.2 Non-linear Topology

The methods introduced so far are limited to linear precision in the characterization of singular points. We saw previously that non-linear critical or degenerate points are unstable. However, when imposed constraints exist (e.g. symmetry or incompressibility of the flow), they can be encountered. To extend existing methods, Scheuermann et al. proposed a scheme for the extraction and visualization of higher-order critical points in two-dimensional vector fields [25]. The basic idea is to identify regions where the index is larger than 1 (or less than -1). In such regions,

the original piecewise linear interpolant is replaced by a polynomial approximating function. The polynomial is designed in Clifford algebra, based on theoretical results presented in [24]. This permits to infer the underlying presence of a critical point with arbitrary complexity that is next modeled and visualized as shown in Fig. 9. An alternative way to replace several close linear singularities by a higher-order one

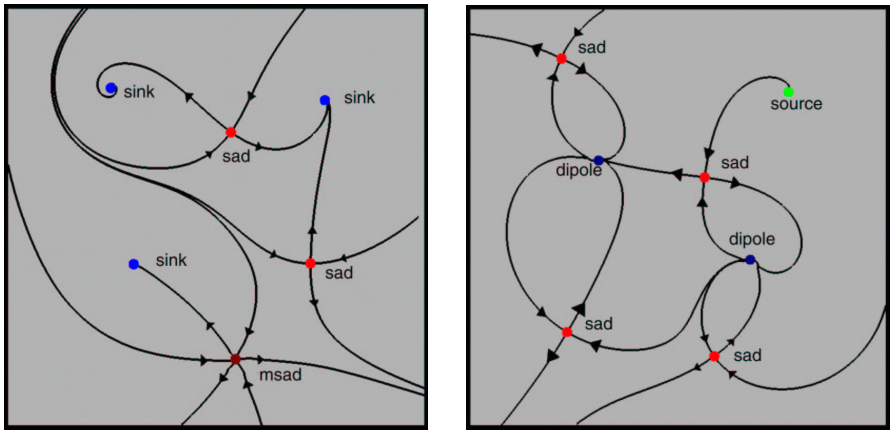

Figure 9: Non-linear topologies

is suggested by Tricoche et al. in [29]. It works with local grid deformations and can be applied to both planar vector and tensor fields. Moreover, it ensures continuity over the whole domain.Based on an analoguous mathematical background as [25], Mann and Rockwood presented a scheme for the detection of arbitrary critical points in 3D [17]. Geometric Algebra is used to compute the 3D index of a vector field, which is obtained as an integral over the surface of a cube. Getting back to the original ideas of Poincaré in his study of dynamical systems, Trotts et al. proposed in [26] a method to extract and visualize the non-linear structure of a "critical point at infinity" when the considered vector field is defined over an unbounded domain.

4.3 Topology Simplification

Topology-based visualization usually results in clear and synthetic depictions that ease analysis and interpretation. Yet turbulent flows, like those encountered in CFD simulations, lead to topologies exhibiting many structures of very small scale. Their proximity and interconnection in the global picture cause visual clutter with classical methods. This drawback is even worsened by low-order interpolation schemes, typical in practice, that confuse the results by introducing artifacts. Therefore, there is a need for post-processing methods that permit to clarify the topologies by emphasizing the most meaningful properties of the flow and suppressing local details and numerical noise. The problem was first addressed by de Leeuw et al. [15] for vector planar fields. Pairs of interconnected critical points are pruned along with the corresponding edges while preserving consistency. The importance of sinks and sources

is evaluated with respect to the surface of their inflow (resp. outflow) regions. Since the method is graph-based the resulting simplified topology lacks a corresponding vector field description. Tricoche et al. proposed an alternative approach for both

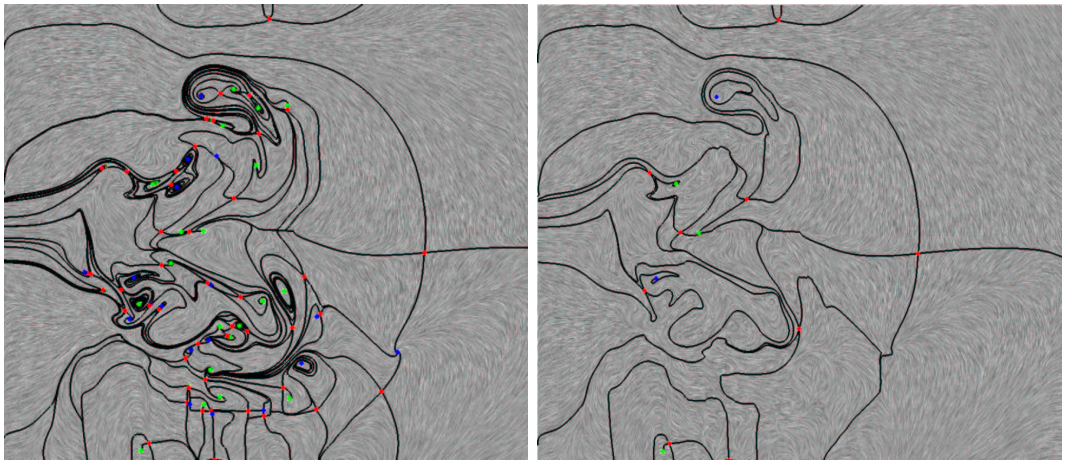

Figure 10: Turbulent and simplified topologies

vector and tensor fields defined in the plane [29]. Close singularities are merged, resulting in a higher order singularity that synthesizes the structural impact of small scale features in the large. This reduces the number of singular points as well as the global complexity of the graph. The merging effect is achieved by local grid deformations that modify the vector field. There is no assumption about grid structure or interpolation scheme. The same authors presented a second method that works directly on the discrete values defined at the vertices of a triangulation [31]. Angle constraints drive a local modification of the vector field that removes pairs of singularities of opposite indices. This simulates a fold bifurcation. Results are shown in Fig. 10 for a vortex breakdown simulation. A major advantage compared to the previous method is that the simplification process can be controled not only by geometric considerations by also by arbitrary user-prescribed criteria (qualitative or quantitative, local or region-based), specific to the considered application.

4.4 Topology Tracking

Theoretical results show that bifurcations are the key to understand and thus properly visualize parameter-dependent flow fields: they transform the topology and explain how the stable structures arise that are observed for discrete values of the parameter. Typical examples in practice are time-dependent datasets. This basic observation motivates the design of techniques that permit to accurately visualize the continuous evolution of topology. A first attempt was the method proposed by Helman and Hesselink in [10]. The one-dimensional parameter space is displayed as third dimension (2D vector fields). However, the method is restricted to a graphical

connection between the successive positions of critical points and associated sepatrices, leading to a ribbon if consistency was preserved. Thus, no connection is made if a structural transition has occured: bifurcations are missed. The same restriction holds for the transposition of this technique to tensor fields by Delmarcelle and Hesselink [6]. Tricoche et al. attacked this deficiency in [32, 30]. The central idea of their technique is to handle the mathematical space, made of the euclidean space on one hand and the parameter space on the other hand, as a continuum. The vector or tensor data are supposed to lie on a triangulation that remains constant. A "space-time" grid is constructed by linking corresponding triangles through prisms over the parameter space. The choice of a suitable interpolation scheme permits an accurate and efficient tracking of singular points through the grid along with the detection of local bifurcations on the way. Including the scheme of [34], closed orbits are tracked in a similar way. Again, the technique results in a 3D representation. The paths followed by critical points are depicted as curves. Separatrices integrated from saddles and closed orbits span smooth separating surfaces. These surfaces are used further to detect modifications in the global topological connectivity: consistency breaks correspond to global bifurcations. Examples are proposed in Fig. 11.

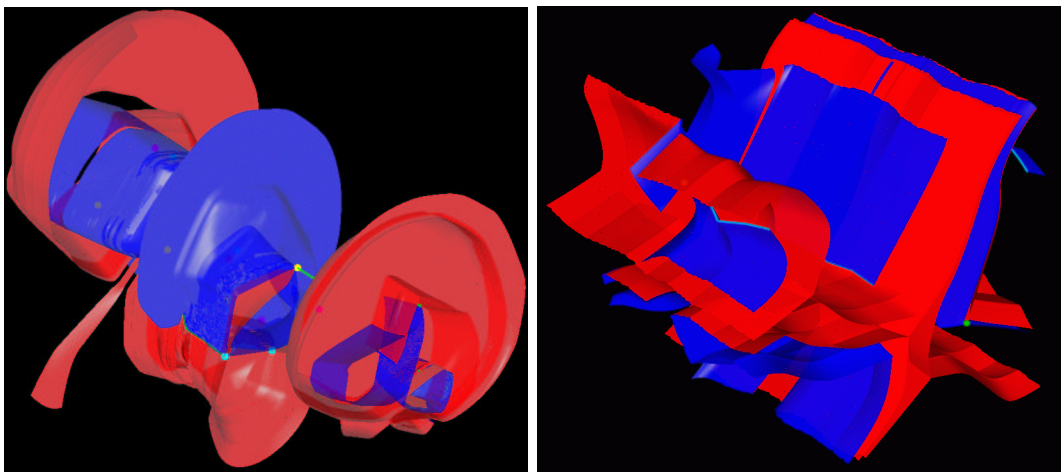

Figure 11: Unsteady vector and tensor topologies

5 Future Research

So far, the major limitation of many existing topological methods is their restriction to two-dimensional datasets. This is especially true in the case of tensor fields. In fact, the basic idea behind topology, i.e. the structural partition of a flow into regions of homogenous behaviour, is definitely not restricted to 2D. However, the theoretical framework requires further research effort to serve as a basis for 3D visualization

techniques. Now, in the simple case of linear precision in the characterization of critical points, topology-based visualization of 3D vector fields still lacks a fast, accurate and robust technique to compute separating surfaces. This becomes challenging in regions of strong vorticity or in the vicinity of critical points, in particular for turbulent flows. In addition, topology-based visualization of parameter-dependent, 3D fields must overcome the limitations inherent to human beings in apprehending the information contained in 4D datasets.

Dealing with time-dependent vector fields, there is a fundamental issue with topology. The technique described in section 4.4 addresses the visualization of the unsteady streamlines' topology. Remember that streamlines are defined as integral curves in steady vector fields. In the context of time-dependent vector fields, they must be thought of as instantaneous integral curves, that is the path of particules that circulate with infinite speed. This might sound a weird idea. Actually, this is a typical way for fluid dynamicists to investigate the structure of time-dependent vector fields in practice. Observe that there is no restriction to this technique for the visualization of parameter-dependent vector fields, this parameter not being time. Nevertheless, if one is interested in the structure of path lines, that is the paths of particles that flow under the influence of a vector field varying over time, one has to rethink the notion of topology. As a matter of fact, the asymptotic behaviour of path lines is not relevant for analysis since there is no longer infinite time for them to converge toward critical points. Thus, a new approach is required to define "interesting" behaviours. Furthermore, a structural equivalence relation must be determined between path lines, upon which a corresponding topology can be built. This seems to be a promising research direction, both from a theoretical and practical viewpoint, to extend the scope of topological methods in the future.

References

[1] Andronov, A. A., Leontovich, E. A., Gordon, I. I., Maier, A. G., *Qualitative Theory of Second-Order Dynamic Systems.* Israel Program for Scientific Translations, Jerusalem, 1973.

[2] Abraham, R. H., Shaw, C. D., *Dynamics, the Geometry of Behaviour I-IV.* Aerial Press, Santa Cruz (Ca), 1982, 1983, 1985, 1988.

[3] Chong, M. S., Perry, A. E., Cantwell, B. J., *A General Classification of Three-Dimensional Flow Fields.* Physics of Fluids, Vol. A2(5), 1990, pp. 765-777.

[4] Dallmann, U., *Topological Structures of Three-Dimensional Flow Separations.* DFVLR-AVA Bericht Nr. 221-82 A 07, Deutsche Forschungs- und Versuchsanstalt für Luft- und Raumgfahrt e.V., April 1983.

[5] Delmarcelle, T., *The Visualization of Second-Order Tensor Fields.* PhD Thesis, Stanford University, 1994.

[6] Delmarcelle, T., Hesselink, L., *The Topology of Symmetric, Second-Order Tensor Fields.* IEEE Visualization '94 Proceedings, IEEE Computer Society Press, Los Alamitos, 1994, pp. 140-147.

[7] Guckenheimer, J., Holmes, P., *Nonlinear Oszillations, Dynamical Systems and Linear Algebra.* Springer, New York, 1983.

[8] Globus, A., Levit, C., Lasinski, T., *A Tool for the Topology of Three-Dimensional Vector Fields.* IEEE Visualization '91 Proceedings, IEEE Computer Society Press, Los Alamitos, 1991, pp. 33-40.

[9] Helman, J. L., Hesselink, L., *Representation and Display of Vector Field Topology in Fluid Flow Data Sets.* Computer, Vol. 22, No. 8, 1989, pp. 27-36.

[10] Helman, J. L., Hesselink, L., *Visualizing Vector Field Topology in Fluid Flows.* IEEE Computer Graphics and Applications, Vol. 11,No. 3, 1991, pp. 36-46.

[11] Hesselink, L., Levy, Y., Lavin, Y., *The Topology of Symmetric, Second-Order 3D Tensor Fields.* IEEE Transactions on Visualization and Computer Graphics, Vol. 3, No. 1, 1997, pp. 1-11.

[12] Hirsch, M. W., Smale, S., *Differential Equations, Dynamical Systems and Linear Algebra.* Academic Press, New York, 1974.

[13] Hultquist, J. P. M., *Constructing Stream Surfaces in Steady 3D Vector Fields.* IEEE Visualization '92 Proceedings, IEEE Computer Society Press, Los Alamitos, 1992, pp. 171-178.

[14] Lighthill, M. J., *Attachment and Separation in Three Dimensional Flow.* L. Rosenhead, Laminar Boundary Layers II, Oxford University Press, Oxford, 1963, pp. 72-82.

[15] de Leeuw, W. C., van Liere, R., *Collapsing Flow Topology Using Area Metrics* IEEE Visualization '99 Proceedings, IEEE Computer Society Press, Los Alamitos, 1999, pp. 349-354.

[16] Lavin, Y., Levy, Y., Hesselink, L., *Singularities in Nonuniform Tensor Fields.* IEEE Visualization '97 Proceedings, IEEE Computer Society Press, Los Alamitos, 1997, pp. 59-66.

[17] Mann, S., Rockwood, A., *Computing Singularities of 3D Vector Fields with Geometric Algebra.* IEEE Visualization '02, IEEE Computer Society Press, Los Alamitos, 2002, pp. 283-289.

[18] Nielson, G. M., Jung, I.-H., *Tools for Computing Tangent Curves for Linearly Varying Vector Fields over Tetrahedral Domains.* IEEE Transactions on Visualization and Computer Graphics, Vol. 5, No. 4, 1999, pp. 360-372.

[19] Perry, A. E., Chong, M. S., *A description of eddying motions and flow patterns using critical point concepts.* Ann. Rev. Fluid Mech., 1987, pp. 127-155.

[20] Poincaré, H., *Sur les courbes définies par une équation différentielle.* J. Math. 1, 1875, pp. 167-244. J. Math. 2, 1876, pp. 151-217. J. Math. 7, 1881, pp. 375-422. J. Math. 8, 1882, pp. 251-296.

[21] Press, W. H., Teukolsky, S. A., Vetterling, W. T., Flannery, B. P., *Numerical Recipes in C.* (2nd ed.) Cambridge, Cambridge University Press, 1992.

[22] Scheuermann, G., Bobach, T., Hagen, H., Mahrous, K., Hahmann, B., Joy, K. I., Kollmann, W., *A Tetrahedra-Based Stream Surface Algorithm.* IEEE Visualization '01 Proceedings, IEEE Computer Society Press, Los Alamitos, 2001.

[23] Scheuermann, G., Hamann, B., Joy, K. I., Kollmann, W., *Visualizing Local Topology.* Journal of Electronic Imaging 9(4), October 2000.

[24] Scheuermann G., Hagen H., Krüger H., *An interesting class of polynomial vector fields.* In Morton Daehlen, Tom Lyche, Larry L. Schumaker (eds.), Mathematical Methods for Curves and Surfaces II, Vanderbilt University Press, Nashville, 1998, pp. 429-436.

[25] Scheuermann, G., Krüger, H., Menzel, M., Rockwood, A. P., *Visualizing Nonlinear Vector Field Topology.* IEEE Transactions on Visualization and Computer Graphics, Vol. 4, No. 2, 1998, pp. 109-116.

[26] Trotts, I., Kenwright, D., Haimes, R., *Critical Points at Infinity: A Missing Link In Vector Field Topology.* NSF/DoE Lake Tahoe Workshop on Hierarchical Approximation and Geometrical Methods for Scientific Visualization, October 2000.

[27] Tobak, M., Peake, D. J., *Topology of three-dimensional separated flows.* Ann. Rev. Fluid Mechanics, Vol. 14, 1982, pp. 81-85.

[28] Tricoche, X., *Vector and Tensor Topology Simplification, Tracking, and Visualization.* Ph.D. thesis, Schriftenreihe FB Informatik 3, University of Kaiserslautern, Germany, 2002.

[29] Tricoche, X., Scheuermann, G., Hagen, H., *Vector and Tensor Field Topology Simplification on Irregular Grids.* Data Visualization 2001 - Proceedings of the Joint Eurographics - IEEE TCVG Symposium on Visualization, Springer, Wien, 2001, pp. 107-116.

[30] Tricoche, X., Scheuermann, G., Hagen, H., *Tensor Topology Tracking: A Visualization Method for Time-Dependent 2D Symmetric Tensor Fields.* Eurographics '01 Proceedings, Computer Graphics Forum 20(3), September 2001, pp. 461-470.

[31] Tricoche, X., Scheuermann, G., Hagen, H., *Continuous Topology Simplification of 2D Vector Fields.* IEEE Visualization '01 Proceedings, IEEE Computer Society Press, Los Alamitos, 2001.

[32] Tricoche, X., Wischgoll, T., Scheuermann, G., Hagen, H., *Topology Tracking for the Visualization of Time-Dependent Two-Dimensional Flows.* Computers & Graphics 26, 2002, pp. 249-257.

[33] Westermann, R., Johnson, C., Ertl, T., *Topology-Preserving Smoothing of Vector Fields.* IEEE Transactions on Visualization and Computer Graphics, 7(3), July-September 2001, pp. 222-229.

[34] Wischgoll, T., Scheuermann, G., *Detection and Visualization of Closed Streamlines in Planar Flows.* IEEE Transactions on Visualization and Computer Graphics 7(2), June 2001, pp. 165-172.

[35] Wischgoll, T., Scheuermann, G., *3D Loop Detection and Visualization in Vector Fields.* To appear in "Mathematical Visualization" (Vismath 2002 Proceedings), 2003.